Available online at www.sciencedirect.com
SCIENCE DIRECT
European Journal of Mechanics B/Fluids 24 (2005) 189–203

Steady states, oscillations and heat explosion in a combustion problem with convection

A. Lazarovici [a], V. Volpert [b], J.H. Merkin [a,*]

[a] *Department of Applied Mathematics, University of Leeds, Leeds LS2 9JT, UK*
[b] *Laboratoire MAPLY, univ. Lyon I, bat. 101, 43, bd du 11 Novembre 1918, 69622 Villeurbanne cedex, France*

Received 8 December 2003; received in revised form 12 June 2004; accepted 23 June 2004

Available online 10 August 2004

Abstract

The effect of convection on the heat generated by an exothermic reaction is considered within a square reactor bounded by constant temperature walls. The fluid flow and heat transfer equations are solved numerically for a range of values of the Rayleigh *Ra* and Frank-Kamenetskii K numbers. From these solutions, boundaries between bounded solutions and thermal runaway are determined, with the range of K for bounded solutions increasing as *Ra* is increased. The system is capable of sustaining both steady and oscillatory behaviour, including simple periodic as well as both chaotic and period-three responses. A parametric region where there is hysteresis is found with either oscillations or steady states seen at the same parameter values, dependent on the initial configuration of the system.

Keywords: Combustion; Natural convection; Thermal runaway; Oscillatory convection; Aperiodic response

1. Introduction

Thermal runaway occurs when the build up of heat released by one or more exothermic reactions overcomes heat losses to the environment or to other endothermic processes. The result is a thermal explosion and it is clearly of considerable importance to determine the critical conditions differentiating between those cases when heat loss can control the heat release and when it fails to do so. Perhaps the simplest model to describe this behaviour is due to Semenov [1] which can be represented by the single equation

$$\frac{\mathrm{d}\theta}{\mathrm{d}t} = K\,\mathrm{e}^{\theta} - \theta, \tag{1}$$

where the term e^{θ} arises from a simplification of Arrhenius kinetics (the exponential approximation) and K is the Frank-Kamenetskii parameter and is a measure of the heat produced by the reaction relative to its loss by Newtonian cooling. Eq. (1) has a critical value K_{crit} for K such that, for $K < K_{\mathrm{crit}}$, the temperature θ remains bounded for all times (at least from reasonable starting conditions), whereas, for $K > K_{\mathrm{crit}}$, θ becomes infinite at a finite time. (In this simple model $K_{\mathrm{crit}} = \mathrm{e}^{-1}$.)

* Corresponding author. Tel.: +44-113-343-5108; fax: +44-113-343-5090.
E-mail address: amtjhm@maths.leeds.ac.uk (J.H. Merkin).

0997-7546/$ – see front matter
doi:10.1016/j.euromechflu.2004.06.007

A generalization of this simple model is to assume that the temperature also has some spatial variation, with heat now being lost by heat transfer across the boundaries of the reaction region. The model becomes, in its simplest form,

$$\frac{\partial\theta}{\partial t} = \nabla^2\theta + K\,\mathrm{e}^{\theta} \tag{2}$$

in a bounded region Ω, with some conditions on θ given on the boundary $\partial\Omega$ of Ω. Systems of this type also exhibit criticality with the value of K_{crit} being dependent both on the geometrical form that Ω takes and the nature of the boundary conditions prescribed on $\partial\Omega$ [2,3]. In both models (1), (2) the consumption of reactants is ignored. This can sometimes have a controlling influence on thermal runaway and thus have significant effects on the critical values of Frank-Kamenetskii or Damköhler numbers [4–7].

In situations envisaged by model (2) large temperature gradients can occur within the reaction region Ω. These set up natural convection currents which, in turn, modify both the rate at which heat is generated by the reaction and the heat transfer at the boundaries. The result can be significant changes in the critical parameter values from those that would have been estimated if convection were ignored [9,8]. This has been established in [10,11] where it was shown that the effect is strongly dependent on the nature of the temperature conditions applied on the boundary.

Here we extend the previous analysis [10,11] to the case where all the boundaries are isothermal, i.e. maintained at the same constant (ambient) temperature. Our main aim is to determine the values of the (dimensionless) parameters at which thermal explosion occurs. However, we find that the progress towards criticality from simple steady states to finite-time blowup as one of the system parameters is increased can be through periodic spatio-temporal behaviour (either simple or more complex oscillations). We also find parameter domains where hysteresis occurs, there, for the same parameter values, the system can be either oscillatory or steady depending on the initial start up.

We start by deriving our model, identifying clearly the assumptions made, before briefly outlining our numerical procedure. We then describe our numerical results paying particular attention to how the solution evolves as the Rayleigh and Frank-Kamenetskii numbers increase.

2. Model

We consider a simple first-order exothermic reaction

$$A \to B + \text{heat}, \qquad \text{rate} = k_0 a\,\mathrm{e}^{-E/RT}, \tag{3}$$

where T is the temperature and k_0 the pre-exponential factor, E the activation energy and R the universal gas constant. a is the concentration of reactant A which is assumed to be in sufficient supply to remain constant throughout. For the fluid flow we make the standard Boussinesq approximation, assuming that changes in density ρ can be ignored except in the buoyancy force. Consequent on this is the assumption of constant fluid properties. This leads to the equations for our model as [12]

$$\begin{aligned}
&\operatorname{div}\mathbf{u} = 0,\\
&\frac{\partial\mathbf{u}}{\partial t} + \mathbf{u}\cdot\nabla\mathbf{u} = -\frac{1}{\rho}\nabla p + g\beta(T - T_0)\mathbf{j} + \nu\nabla^2\mathbf{u},\\
&\frac{\partial T}{\partial t} + \mathbf{u}\cdot\nabla T = \kappa\nabla^2 T + Qk_0 a\,\mathrm{e}^{-E/RT},
\end{aligned} \tag{4}$$

where $\mathbf{u}$ is the fluid velocity field and p is the pressure. κ and ν are the thermometric conductivity and kinematic viscosity respectively, Q is the exothermicity factor and g is the acceleration due to gravity, with $\mathbf{j}$ a unit vector in the vertical direction.

Eqs. (4) are to be solved on the square 2D region of side ℓ, namely on $0 < x < \ell$, $0 < y < \ell$, where x and y are, respectively, horizontal and vertical Cartesian co-ordinates with corresponding velocity components (u, v). $T = T_0$ (T_0 constant) on the boundaries, where we also apply the no-slip conditions on $\mathbf{u}$.

We make Eqs. (4) dimensionless by introducing the variables

$$\theta = \frac{E(T - T_0)}{RT_0^2}, \quad t = \frac{\ell^2}{\kappa}\bar{t}, \quad (x, y) = \ell(\bar{x}, \bar{y}), \quad (u, v) = \frac{\kappa}{\ell}(\bar{u}, \bar{v}), \quad p = \frac{\rho\kappa^2}{\ell^2}\bar{p}, \tag{5}$$

This leads to the dimensionless equations for our model as, on dropping the bars for convenience,

$$\begin{aligned}
\frac{\partial\theta}{\partial t}+u\frac{\partial\theta}{\partial x}+v\frac{\partial\theta}{\partial y} &= \frac{\partial^2\theta}{\partial x^2}+\frac{\partial^2\theta}{\partial y^2}+K\,\mathrm{e}^{\theta},\\
\frac{\partial u}{\partial t}+u\frac{\partial u}{\partial x}+v\frac{\partial u}{\partial y} &= -\frac{\partial p}{\partial x}+\sigma\left(\frac{\partial^2 u}{\partial x^2}+\frac{\partial^2 u}{\partial y^2}\right),\\
\frac{\partial v}{\partial t}+u\frac{\partial v}{\partial x}+v\frac{\partial v}{\partial y} &= -\frac{\partial p}{\partial y}+\sigma\left(\frac{\partial^2 v}{\partial x^2}+\frac{\partial^2 v}{\partial y^2}\right)+\sigma\,Ra\,\theta,\\
\frac{\partial u}{\partial x}+\frac{\partial v}{\partial y} &= 0,
\end{aligned} \tag{6}$$

where $\sigma=\nu/\kappa$ is the Prandtl number, which we set to unity from now on (a reasonable approximation for most gases), and where

$$K=\frac{EQk_0a\,\mathrm{e}^{-E/RT_0}\ell^2}{RT_0^2\kappa},\qquad Ra=\frac{g\beta RT_0^2\ell^3}{E\kappa\nu}$$

are the Frank-Kamenetskii and Rayleigh numbers respectively (β is the coefficient of thermal expansion). We have also made the exponential approximation in the equation for θ, essentially assuming that $RT_0/E\ll 1$.

The boundary conditions to be applied are that

$$\theta=0,\quad u=v=0\quad \text{on } x=0,1\ (0\leqslant y\leqslant 1),\ \text{and } y=0,1\ (0\leqslant x\leqslant 1). \tag{7}$$

3. Numerical method

We use the vorticity–stream function approach for the numerical computations, defining stream function ψ and vorticity ω such that

$$u=\frac{\partial\psi}{\partial y},\qquad v=-\frac{\partial\psi}{\partial x},\qquad \omega=-\nabla^2\psi. \tag{8}$$

Substituting ψ and ω into Eqs. (6) we obtain

$$\begin{aligned}
\frac{\partial\theta}{\partial t}+\frac{\partial\psi}{\partial y}\frac{\partial\theta}{\partial x}-\frac{\partial\psi}{\partial x}\frac{\partial\theta}{\partial y} &= \nabla^2\theta+K\,\mathrm{e}^{\theta},\\
\frac{\partial\omega}{\partial t}+\frac{\partial\psi}{\partial y}\frac{\partial\omega}{\partial x}-\frac{\partial\psi}{\partial x}\frac{\partial\omega}{\partial y} &= \sigma\nabla^2\omega+\sigma\,Ra\,\frac{\partial\theta}{\partial x},\\
-\nabla^2\psi &= \omega
\end{aligned} \tag{9}$$

together with the boundary conditions

$$\begin{aligned}
&\theta=0,\quad \psi=0,\quad \frac{\partial\psi}{\partial y}=0\quad \text{on } x=0,1\ (0<y<1),\\
&\theta=0,\quad \psi=0,\quad \frac{\partial\psi}{\partial x}=0\quad \text{on } y=0,1\ (0<x<1).
\end{aligned} \tag{10}$$

No boundary condition is prescribed on the vorticity and, at each time step, the boundary condition on ω is derived from the values of ψ and ω at neighbouring points inside the box computed at the previous time step. We use ψ_1 and ω_1 at the nearest interior point to calculate ω_0, the value of ω on the boundary, from

$$\omega_0=-\frac{\omega_1}{2}-\frac{3\psi_1}{h^2}+\mathrm{O}\big(h^2\big). \tag{11}$$

The numerical method used was an alternating-direction, implicit finite-difference scheme.

For relatively small values of K the system achieves a steady state relatively quickly, even for high values of Ra. We started our numerical computations for a given value of Ra with such a small value of K and its corresponding steady state. We then changed the value of K in small increments, starting the computations with the solution reached at long times for the previous value of K. This process enabled the steady states or periodic behaviour, as appropriate, to be realised relatively quickly so that the computations did not require a long transient period. In some cases, to demonstrate hysteresis, we reduced the value of K starting with a previously calculated solution. Throughout we took $\sigma=1$ and used 40 grid points in the x and y directions ($\Delta x=\Delta y=0.05$).

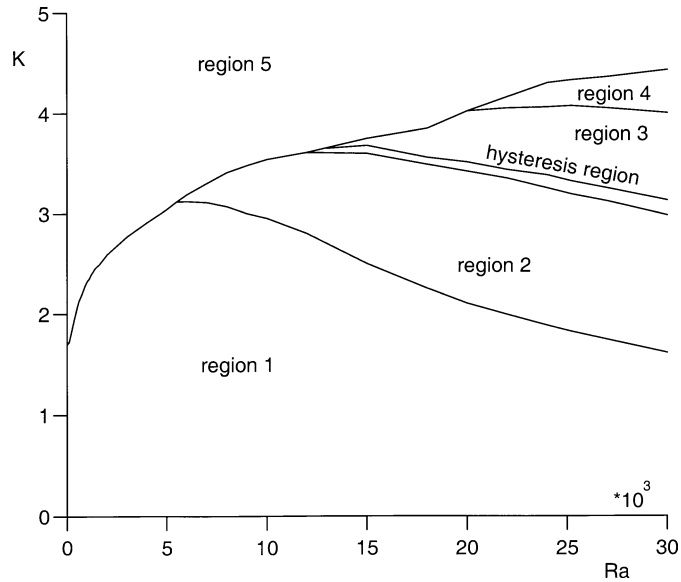

Fig. 1. Explosion limit and convective regions in the (Ra, K) parameter space. Regions 1 and 3 give steady states, regions 2 and 4 give oscillatory behaviour, region 5 gives a heat explosion (finite time blowup in the solution), note the region of hysteresis between regions 2 and 3.

4. Results

The system is known to have two possible basic evolutions depending on the value of the Frank-Kamenetskii number K, either to a steady temperature distribution with convection or to an unbounded growth of the temperature (a finite-time blowup in the solution), called a thermal explosion. Previous work on related problems [10,11] has shown that for systems with weak convective effects ($Ra \sim 10$) explosions occur at relatively small values of K. When the convective effects are stronger ($Ra \sim 10^4$, say) stationary solutions are possible for higher values of K. The reason for this is that the increased heat loss at the boundaries caused by the stronger convection limits the growth of the maximum temperature within the reaction region and thus prevents thermal runaway. Much stronger heat generation by the reaction (higher values of K) are thus required to overcome the stronger heat losses at the boundaries.

We start by considering the (Ra, K) parameter space for our model (Fig. 1). We find that there are five main regions giving qualitatively different behaviour. Regions 1 and 3 correspond to values of Ra and K for which steady solutions exist. Regions 2 and 4 correspond to bounded oscillatory solutions where the temperature and stream function distributions change with time in a periodic (or in an aperiodic) way. Region 5 corresponds to the non-existence of a long time solution to the problem with thermal runaway at a finite time and heat explosion. We note that there is an interesting phenomenon that takes place in a narrow region between regions 2 and 3, where there is a hysteresis between steady and oscillatory solutions.

We now describe the behaviour in these regions in more detail.

4.1. Steady convective solutions

There are two regions in the (Ra, K) parameter space which give rise to steady convection. The temperature and stream function distributions have qualitatively similar forms in these two regions. The maximum temperature is always on the vertical symmetry axis, but not at equal distances from the top and bottom walls. The effect of convection (increase in Ra) is to move the position of the maximum temperature closer to the top wall of the box. This is clearly seen by comparing Figs. 2(a) (for $Ra = 10$, where the temperature field is symmetric and convective effects are neglible) with Figs. 2(b) (for $Ra = 10^3$) and 2(c) (for $Ra = 2.7 \times 10^4$), all for $K = 1.0$. For the first two values of Ra (Figs. 2(a) and 2(b)) the temperature increases monotonically from the vertical walls to the vertical centre-line. At higher values of Ra (Fig. 2(c)) this is not the case and a temperature higher than that at the centre-line is achieved towards the vertical walls on a horizontal cut through the reactor. There is also evidence of boundary layers developing on the top and side walls for this value of Ra.

The corresponding stream function distributions illustrate the role of the convective flow in the temperature distribution. The stream function plots show two geometrically symmetric vortices of opposite sign one negative (clockwise) on the right and one positive (anticlockwise) on the left. This flow suggests that the heat built up by the reaction in the middle of the domain causes a vertical flow in the centre towards the top wall. This upward movement makes the cooler fluid at the boundaries flow downwards

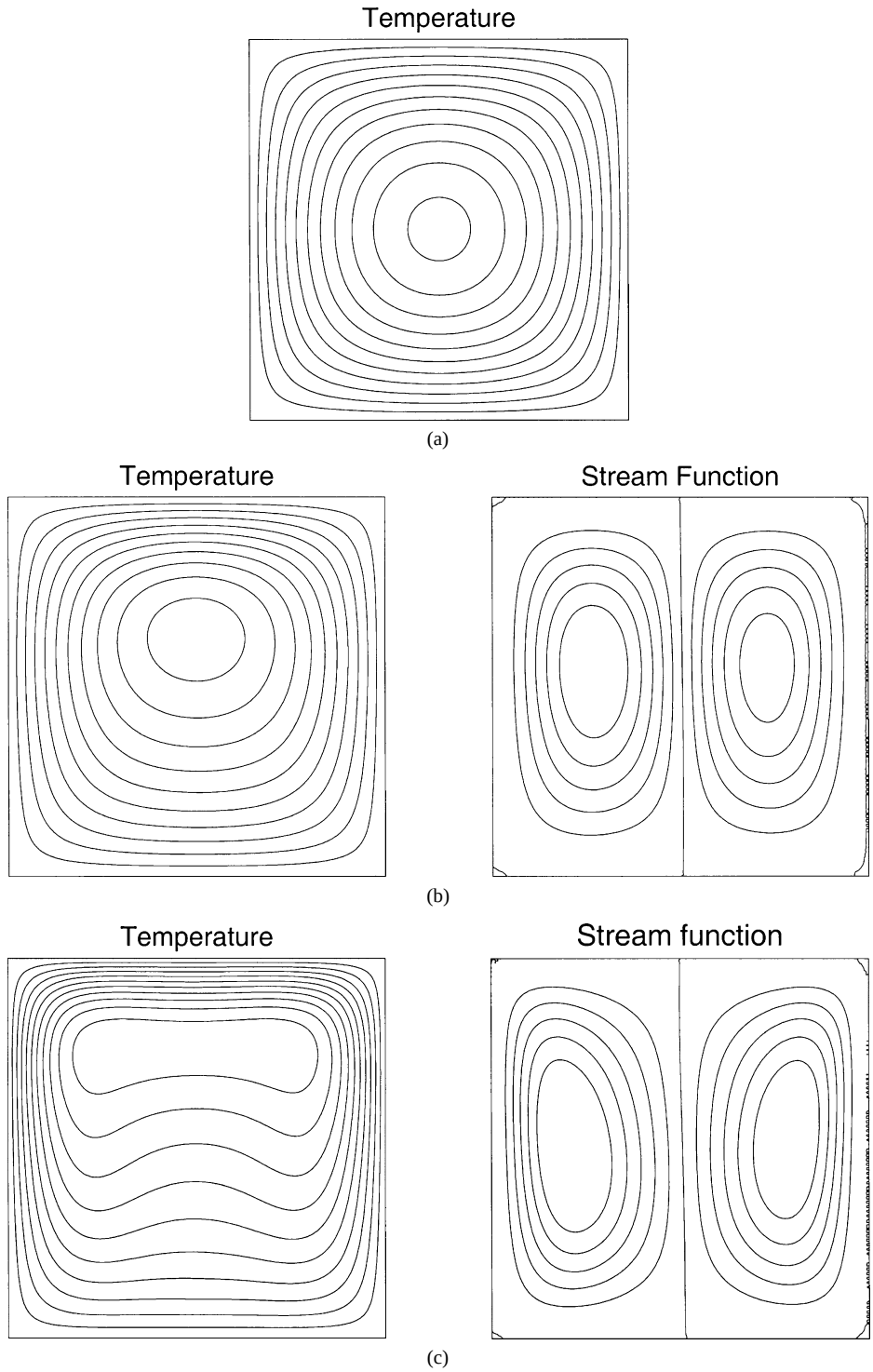

Fig. 2. Contour plots of the temperature and stream function distributions obtained from the numerical integration of Eqs. (9), (10) for (a) $K = 1.0$, $Ra = 10.0$, (b) $K = 1.0$, $Ra = 1000.0$, (c) $K = 1.0$, $Ra = 2.7 \times 10^4$.

near the vertical walls, thus enhancing the heat loss. This effect becomes more pronounced as Ra increases. For high Ra an upward jet develops in the central region with a corresponding downward flow in boundary layers on the side walls. Almost stagnant regions form between these flows which accounts for the increased temperatures in these regions (see Fig. 2(c)).

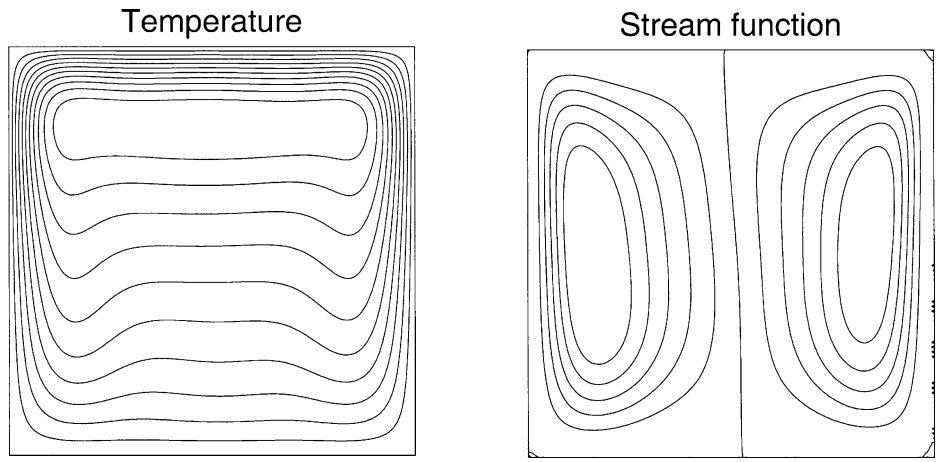

Fig. 3. Contour plots of the temperature and stream function distributions obtained from the numerical integration of Eqs. (9), (10) for $K = 3.5$, $Ra = 2.7 \times 10^4$.

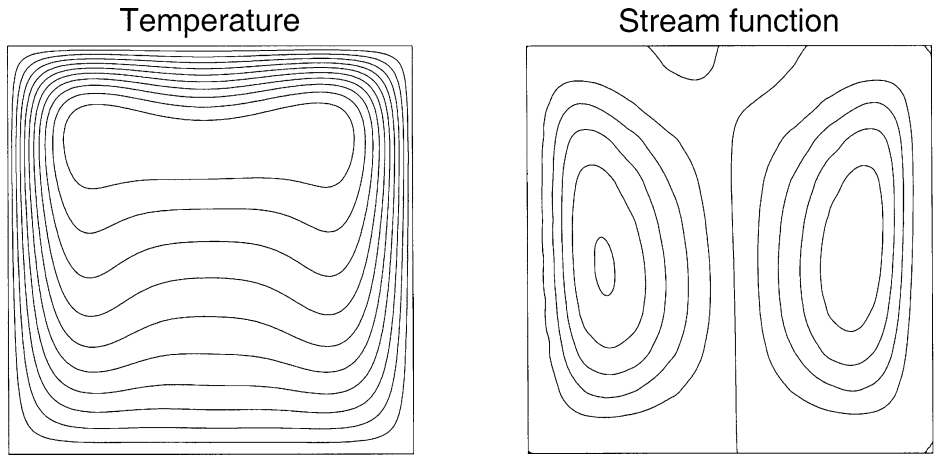

Fig. 4. Contour plots of the temperature and stream function distributions obtained from the numerical integration of Eqs. (9), (10) for $K = 1.73$, $Ra = 2.7 \times 10^4$.

Fig. 2 shows clearly that increasing the convection effects is to reduce the temperatures achieved within the reactor. This can be seen in the changes in the maximum temperature from $T_{\max} = 0.41$ for $Ra = 10^3$ (Fig. 2(b)) to $T_{\max} = 0.22$ for $Ra = 2.7 \times 10^4$ (Fig. 2(c)). There is a corresponding increase in the strength of the flow, with $|\psi_{\max}|$, the maximum value of the stream function, changing from $|\psi_{\max}| = 1.2$ for $Ra = 10^3$ to $|\psi_{\max}| = 5.0$ for $Ra = 2.7 \times 10^4$.

In the second region of steady convection (region 3 in Fig. 1), the increased exothermicity (larger K) accentuates the difference between the temperature distributions for low and high Ra number. Temperature and stream function for $K = 3.5$ and $Ra = 2.7 \times 10^4$ are shown in Fig. 3, to compare with Fig. 2(c). For a given value of Ra, convection is stronger ($|\psi_{\max}| = 7.5$), temperatures are higher ($T_{\max} = 0.99$), and the position of the maximum temperature is closer to the upper wall as the exothermic coefficient K is increased. The development of boundary layers on the upper and side walls is more evident for this higher value of K.

As K is increased for the smaller values of Ra, convection is not strong enough to limit the growth of heat produced in the central part of the reactor and an explosion occurs (thermal runaway at a finite time, region 5 in Fig. 1). In this case the progress is from steady convection to explosion. For higher values of Ra the effects of convection allow the system to progress from steady to oscillatory behaviour as K is increased (before finally having thermal runaway). The way in which steady convection changes before becoming oscillatory is illustrated in Fig. 4, with plots for $K = 1.73$, still with $Ra = 2.7 \times 10^4$. This puts us close to the upper boundary of region 1 in Fig. 1 (similar behaviour is seen close to the upper boundary of region 3). The flow is still steady but the geometric symmetry of the two-vortex stream function pattern is broken, as additional small vortices appear close to the upper wall (where the maximum temperature is located). This increase in K results in increases in temperature

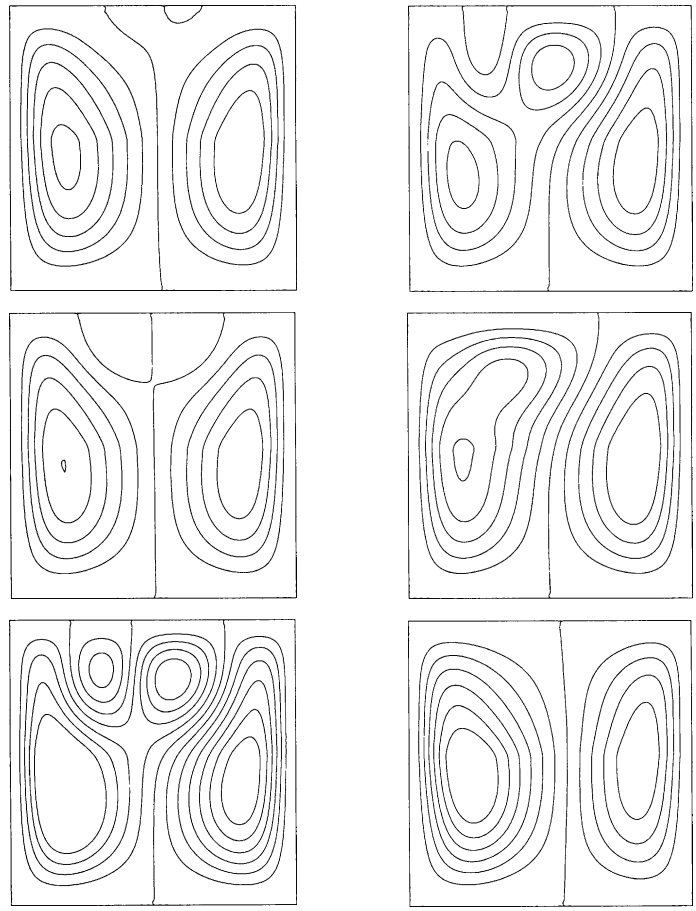

Fig. 5. A sequence of contour plots for the stream function obtained from the numerical integration of Eqs. (9), (10) for $K = 1.76$, $Ra = 2.7 \times 10^4$, showing a period-one oscillatory response.

($T_{\max} = 0.38$) and flow. Since the flow is not now symmetric, the values of the stream function are not symmetric, lying in the range $-6.0 < \psi < 9.0$.

4.2. Oscillatory convective solutions

The move to oscillatory behaviour as K is increased starts with a small vortex appearing towards the centre of the top wall (see Fig. 4). For parameter values still in the steady region (1 or 3), this vortex is steady and of small intensity. As K is increased placing the system just into an oscillatory region (2 or 4), another small vortex (of opposite sign) appears close to the top wall, see Fig. 5 for $K = 1.76$, still with $Ra = 2.7 \times 10^4$. The initially small vortices close to the top wall then increase in size and intensity, displacing the original large vortices. This causes jet-like flows from the central region towards the top corners. The stronger of the two upper vortices then moves towards the centre displacing the weaker vortex, which reduces in size and intensity before disappearing. The remaining upper vortex then merges with lower vortex of the same sign producing an asymmetric, two vortex structure. The asymmetry becomes less pronounced and two, almost symmetric vortices result. This process then repeats with a small vortex again appearing close to the top wall.

The location of the vortices close to the top wall is a consequence of the temperature build-up in this region as can be seen in Fig. 6, which gives temperature plots corresponding to the stream function plots shown in Fig. 5. The temperature distribution starts the oscillatory cycle with a structure similar to that of the steady state (compare with Fig. 4). The appearance of the secondary (initially weak) vortices is to distort the temperature field close to the centre of the top wall, enhancing the heat loss at this wall and thus cooling the fluid in this region. This effect becomes more pronounced as the secondary vortices increase in size and strength. This results in an asymmetry developing in the temperature field and increased cooling in the central region. The effect of the two vortices on the left of the reactor merging is to move the position of the maximum temperature towards the

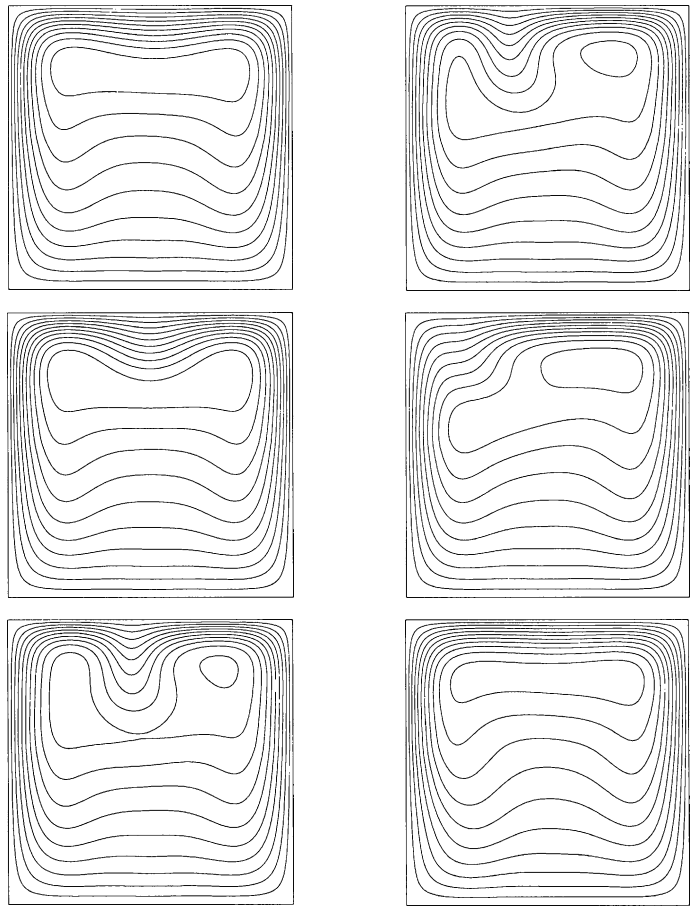

Fig. 6. A sequence of contour plots for the temperature obtained from the numerical integration of Eqs. (9), (10) for $K = 1.76$, $Ra = 2.7 \times 10^4$ (same times as for Fig. 5), showing a period-one oscillatory response.

right-hand corner and to cool the left side of the reactor, where the convective flow is stronger. As the flow symmetry returns so does the symmetry in the temperature field.

The oscillatory sequence given in Figs. 5 and 6 shows simple periodic behaviour. This point is illustrated more clearly in Fig. 7 where we plot the maximum values of the stream function and temperature against t. The stream function plot (Fig. 7(a)) shows a clear period-one response though the temperature plot (Fig. 7(b)) could suggest more complex behaviour. To resolve this point we plotted the corresponding 'limit cycle', i.e. the mean of the temperature distribution against the mean of the stream function values. This is shown in Fig. 7(c) and clearly indicates period-one oscillations. The transition from steady to periodic behaviour is through this period-one response. However, as K is increased (for a given Ra) more complex behaviour is seen.

4.2.1. Complex oscillatory behaviour

As the value of K is increased, still with $Ra = 2.7 \times 10^4$, the amplitude and frequency of the oscillations increase with the response having a more complicated, though still period-one structure. This can be seen in Fig. 8 where we give plots of the maximum temperature against t and the corresponding 'limit cycle' for $K = 2.9$, to compare with Figs. 7(b) and 7(c). As K is increased a little further there is a succession of period doublings, as can be seen in Fig. 9(a) (period-two, for $K = 3.0$), Fig. 9(b) (period-four, for $K = 3.16$) and Fig. 9(c) (period-eight, for $K = 3.179$). Following this there is, perhaps as might be expected, a narrow region of chaotic behaviour. This is illustrated in Fig. 9(d) (for $K = 3.18$) where a weakly chaotic response is seen in the limit cycle. The time trace for this value of K, Fig. 9(e), shows almost periodic behaviour though the power spectrum, Fig. 9(f), does show some spreading of the main peaks arising from the 'periodicity' of the response, suggesting weak chaotic behaviour.

A narrow region of period-three behaviour emerges from the chaotic response as K is increased further, see Fig. 10(a) for $K = 3.21$. A further sequence of period doublings then follows, Fig. 10(b) for $K = 3.231$ and Fig. 10(c) for $K = 3.2312$ before

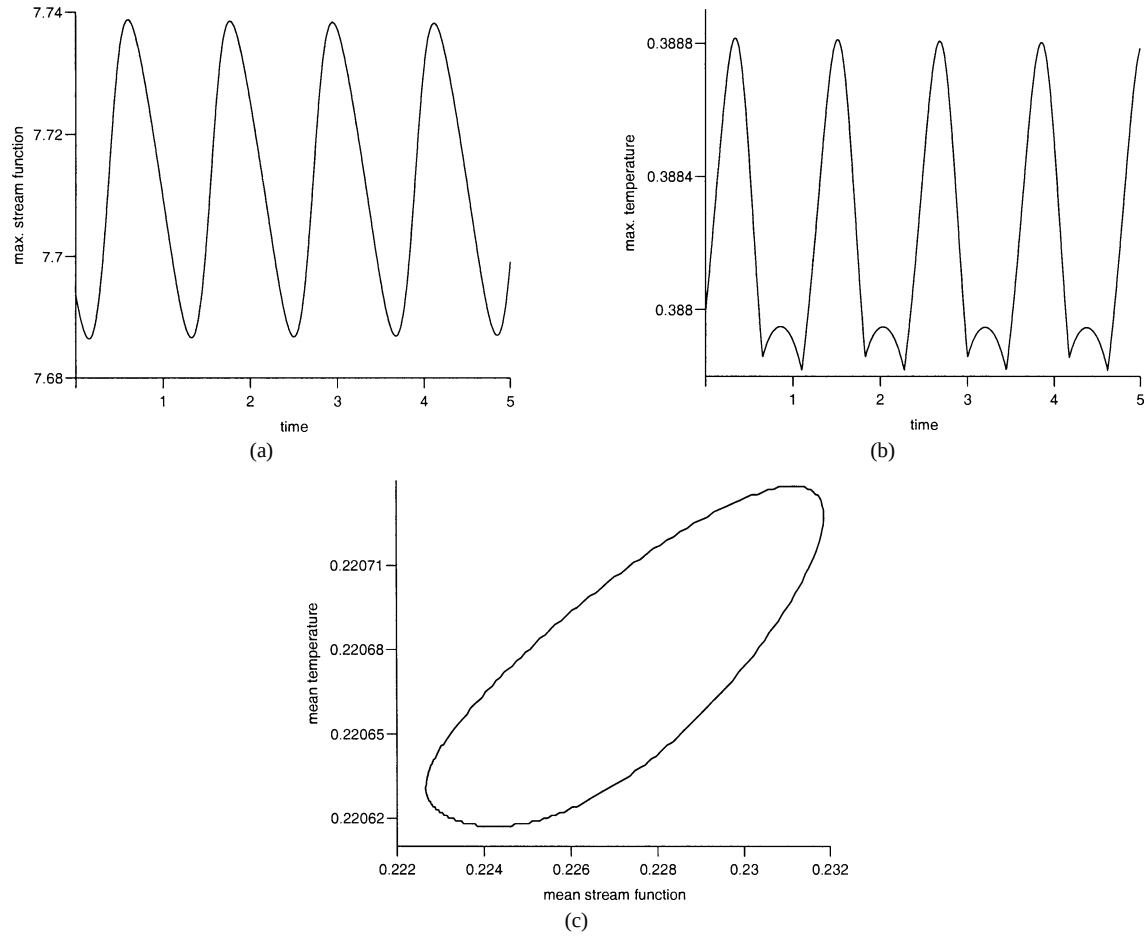

Fig. 7. Graphs of the maximum values of (a) the stream function and (b) temperature against t, (c) the corresponding 'limit cycle', for $K = 1.76$, $Ra = 2.7 \times 10^4$.

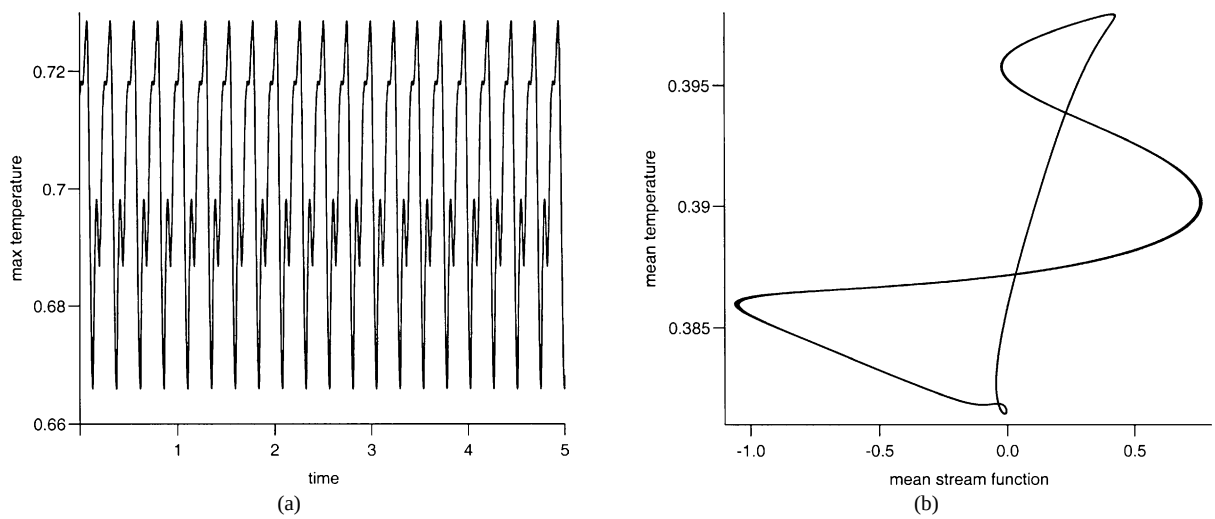

Fig. 8. Graphs of (a) the maximum values of the temperature against t and (b) the corresponding 'limit cycle', for $K = 2.9$, $Ra = 2.7 \times 10^4$, showing a period-one response.

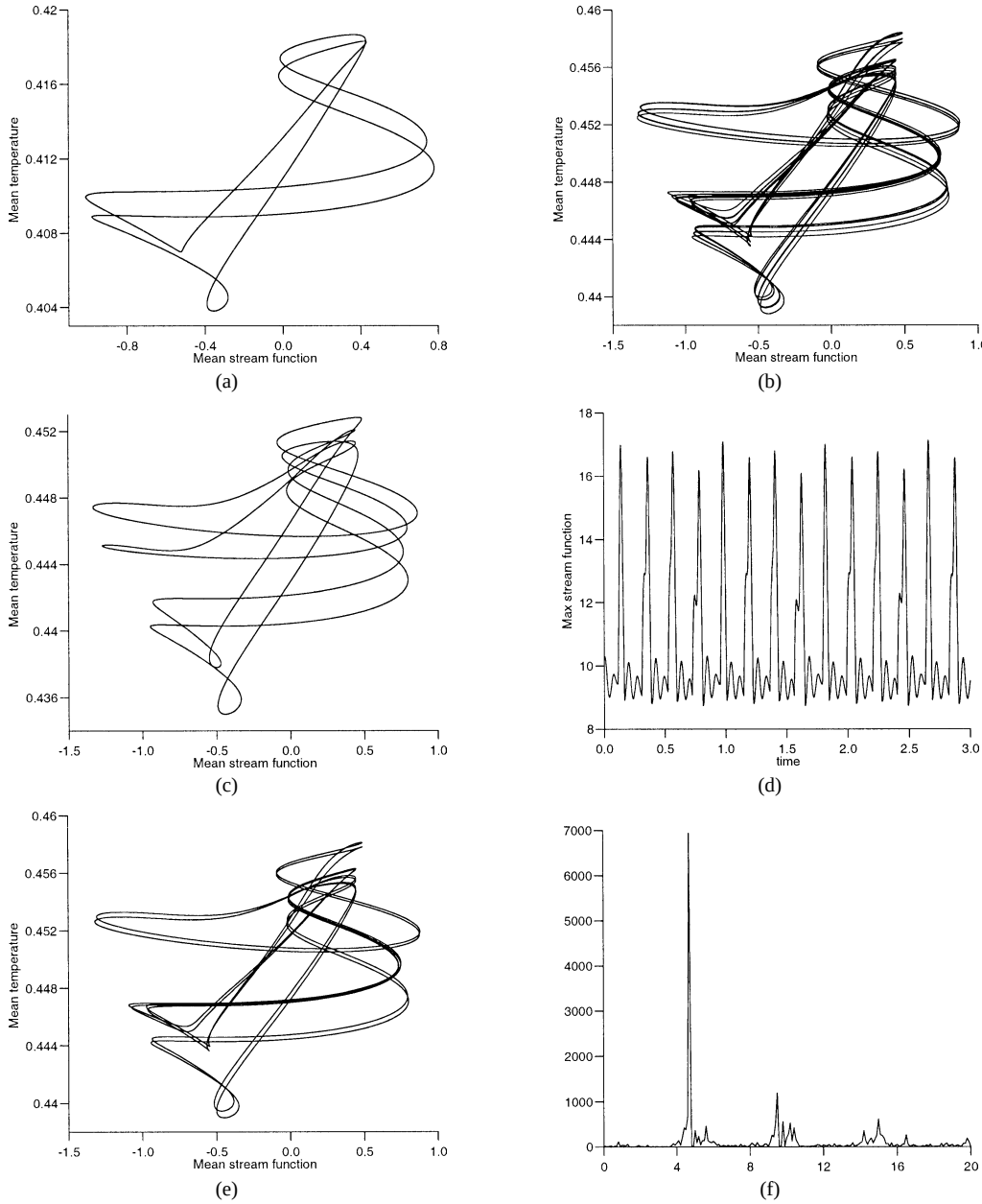

Fig. 9. 'Limit cycles' for $Ra = 2.7 \times 10^4$ and (a) $K = 3.0$, period-two, (b) $K = 3.16$, period-four, (c) $K = 3.179$, period-eight, (e) $K = 3.18$, chaotic response. (d) time trace and (f) power spectrum for $K = 3.18$.

there is another region of chaotic behaviour, Fig. 11 for $K = 3.24$. In this case the chaos is much stronger than that shown in Figs. 9(d)–(f). The time trace, Fig. 11(b), appears much less repetetive and the power spectrum, Fig. 11(c), is much more typical of strongly chaotic behaviour. This value of K is close to the upper limit of region 2 (in Fig. 1) and simpler oscillatory responses return in the hysteresis region (see below) as K is increased further, with the system becoming steady again as the value of K crosses into region 3.

The oscillations in region 4 are similar to those in region 2, with the main difference being that the transition to chaotic behaviour occurs more rapidly as K is increased in this region. This meant that we were unable to locate the period doubling bifurcation points. However, we did locate both period-one and chaotic behaviour, see Figs. 12(a) for $K = 4.06$ and Figs. 12(b) and 12(c) for $K = 4.3$. The upper boundary of this region is the limit of oscillatory explosion.

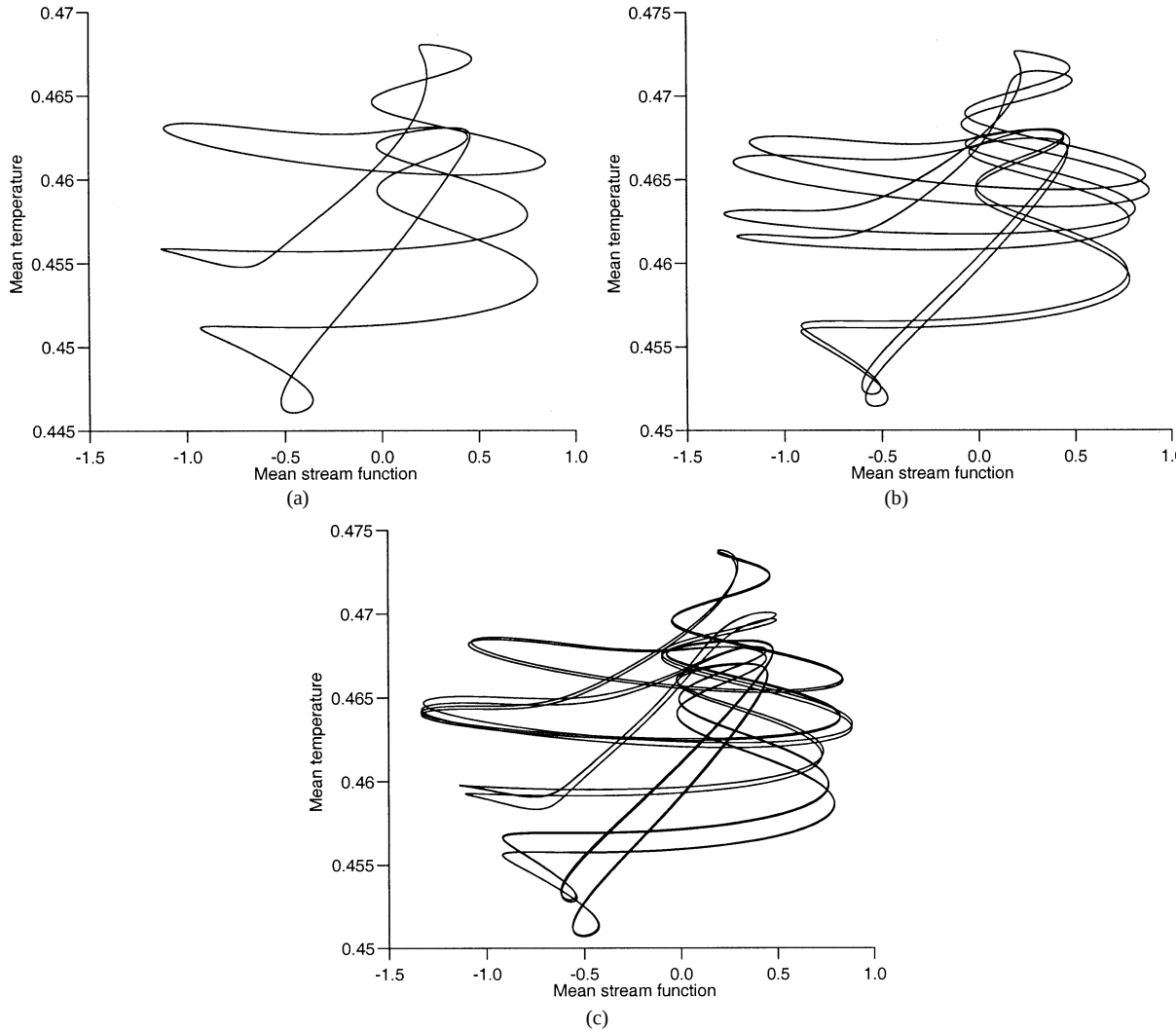

Fig. 10. 'Limit cycles' for $Ra = 2.7 \times 10^4$ and (a) $K = 3.21$, period-three, (b) $K = 3.231$, period-six, (c) $K = 3.2312$, period-twelve.

4.2.2. Complex behaviour: hysteresis

Another feature of the system is the hysteresis of the oscillatory-steady solutions. This occurs in a narrow area between regions 2 and 3 (see Fig. 1). For parameter values in this region, the nature of the solution depends on the initial configuration of the stream function and temperature. For values of K and Ra within this area, if we start with temperature and stream function distributions derived from values of K (and Ra) in the steady region (region 3) then the solution approaches a steady state for that value of K in the hysteresis region. If, however, we start with temperature and stream function distributions derived for an oscillatory solution (region 2) the result is an oscillatory response for the same value of K. We illustrate this in Fig. 13 with plots of the maximum temperature against t for $K = 3.2$, still with $Ra = 2.7 \times 10^4$. The upper curve starts with a higher maximum temperature (from region 3) and quickly approaches a steady value. The lower curve starts with a lower initial value (from region 2) and has a sustained periodic response. There was no sign, within the timeframe of the numerical integrations, of either of these two qualitatively different responses for the same parameter values changing to the other.

4.3. Explosion

Heat explosion occurs if $K > K_{\text{crit}}$. The solution can pass into the explosion region (region 5) with increasing K in two different ways. For parameter values in regions 1 or 3, this transition is from a steady state directly to an explosion. In this case the temperatures within the reactor build up, slowly at first, before increasing very rapidly, finally becoming unbounded

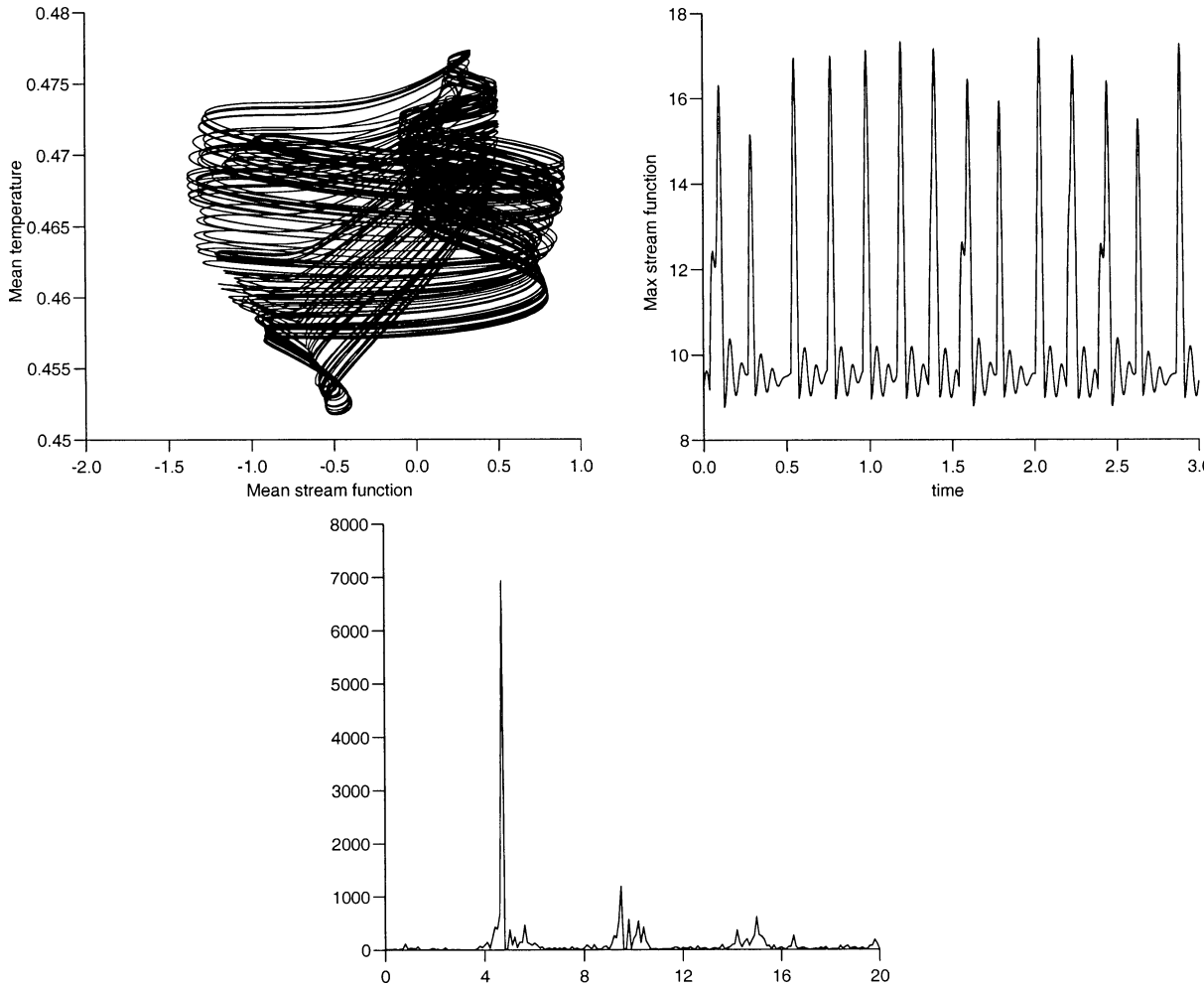

Fig. 11. Chaotic response for $K = 3.24$.

at a finite time. This case is illustrated in Fig. 14(a) for $Ra = 1.7 \times 10^4$, where we show the maximum temperatures plotted against t for $K = 3.7$ (region 3) where the maximum temperature approaches a constant value, and $K = 3.95$ where the maximum temperature blows up at finite time (at $t \simeq 1.62$). Increasing the value of K accelerates the temperature build up and the progress to blowup. This can be seen in Fig. 14(a) by comparing the plots of the maximum temperature for $K = 3.95$ and $K = 4.0$ (blowup at $t \simeq 1.3$). At this point the numerical integration indicates that a singularity is developing in the solution, which breaks down as these high temperatures are approached.

The alternative approach to an explosion is through an oscillatory response becoming unbounded at a finite time. In this case the amplitude of the oscillations increases before the system undergoes an oscillatory explosion. The maximum temperature oscillates, but as it does so, its values become noticeably larger. Soon this growth is accelerated and the temperature builds up quickly leading to a heat explosion. This case is illustrated in Fig. 14(b) for $K = 3.37$, $Ra = 7 \times 10^3$.

5. Conclusions

We have considered the effects that convection can have on the temperature development within a square reactor bounded by isothermal walls resulting from a single first-order exothermic reaction. Our results are presented in terms of the Frank-Kamenetskii K and Rayleigh Ra numbers, which represent the effects of the flow and the exothermicity of the reaction, respectively. Two, qualitatively different types of behaviour are seen. In one, the temperature and flow distributions remain bounded for all time and, in the other, there is a blow up in the solution (explosion) at a finite time. The effect of increasing

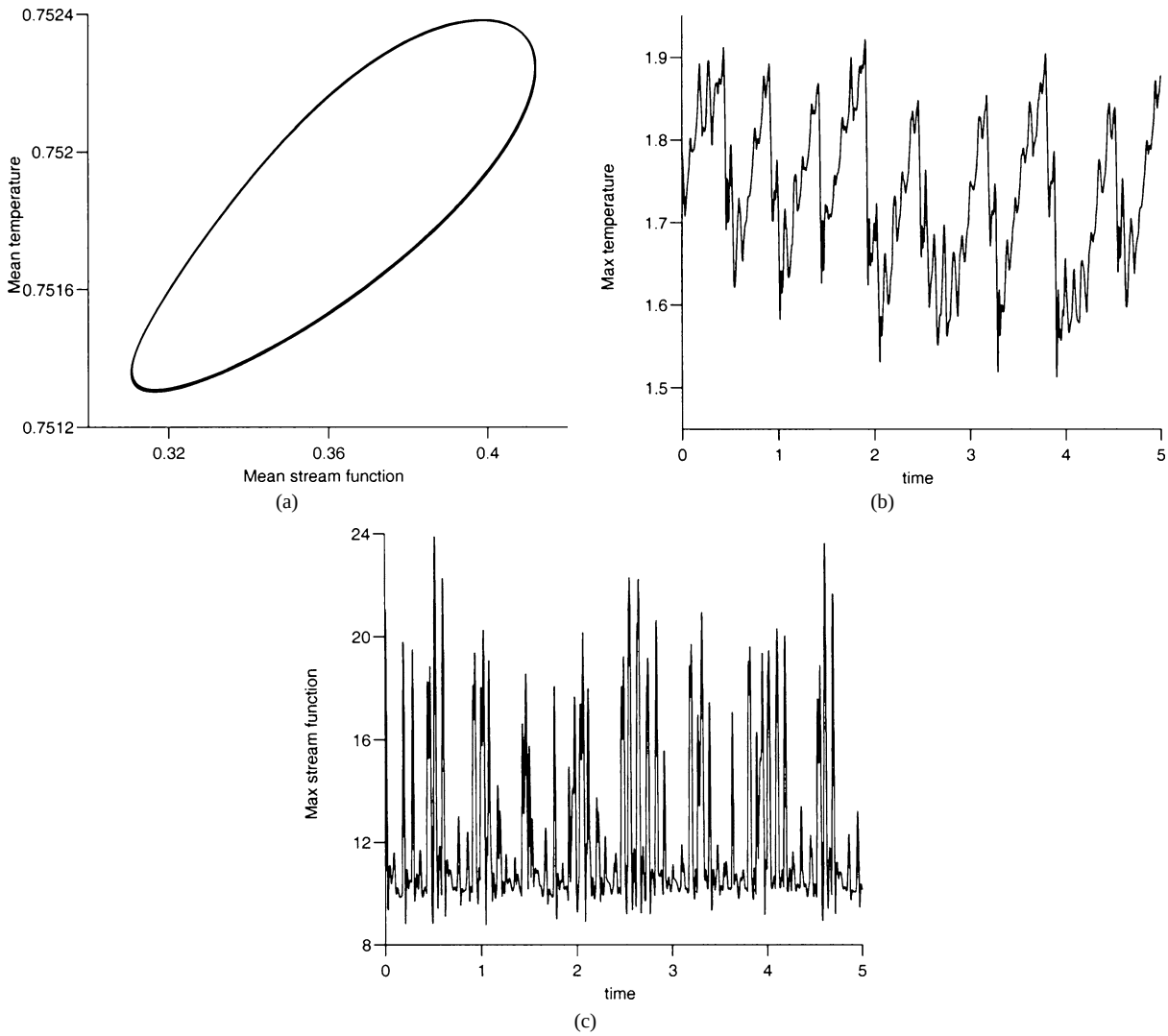

Fig. 12. Graphs of (a) 'limit cycle' for $K = 4.06$, period-one. The maximum values of (b) the stream function and (c) temperature against t, for $K = 4.3$, $Ra = 2.7 \times 10^4$, chaotic response.

Ra (flow effects) is to increase the heat losses at the walls, predominantly at the top and side walls, and thus delay the onset of blowup. Thus bounded behaviour is seen for higher values of K as *Ra* is increased.

The bounded responses include both steady and oscillatory states. The parameter ranges for these have been determined by our numerical simulations, with there being the transition to blow up through both a steady and oscillatory behaviour, as well as transitions between oscillations and steady states (see Fig. 1). We have also identified a parameter region where hysteresis can occur, with both oscillations and a steady state being possible for the same parameter values. Which response is seen depends on the initial condition of the system.

The main effect of the convective flow is to increase heat losses from the walls. Strong convective effects (high *Ra*) can increase this process considerably through boundary layers developing on the top and side walls, see Figs. 2(c), 4–6. Fluid convection takes the hotter fluid generated by the reaction in top part of the reactor to the cooler regions in the bottom part of the reactor, losing heat through the walls as it does so. The consequence is a jet-like upflow in the central part of the reactor of cooler fluid towards the top, where it can be heated by the reaction, and downflows in boundary layers on the walls, where it is cooled.

This interchange of hot and cold fluid can set up steady behaviour or it can be oscillatory, with the flow and temperature distributions changing over a cycle. For most of the parameter values in the oscillatory regions (Fig. 1) these oscillations in the flow and temperature fields are relatively simple in nature, with period-one responses (Fig. 8). However, there are parameter

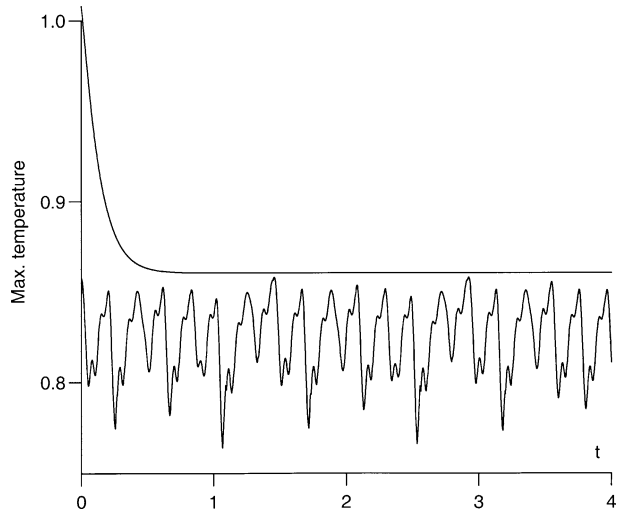

Fig. 13. Graphs of the maximum temperature for $K = 3.2$, $Ra = 2.7 \times 10^4$ in the hysteresis region.

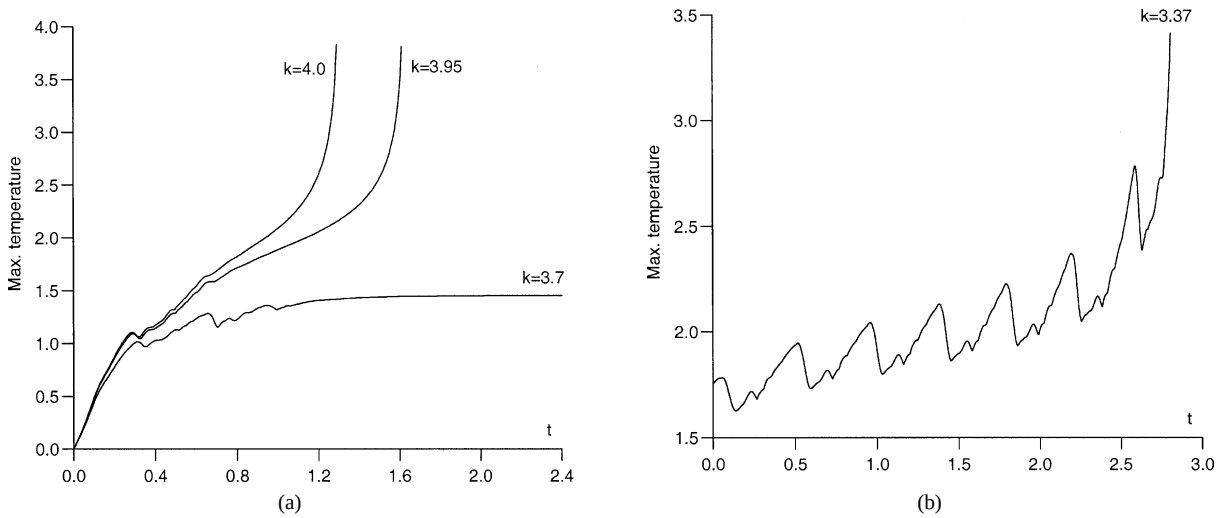

Fig. 14. (a) Maximum temperature plotted against t for $K = 3.7$ (approaches a steady state) and $K = 3.95, 4.0$ (blows up in finite time), $Ra = 1.7 \times 10^4$. (b) Maximum temperature plotted against t for $K = 3.37$ (oscillatory blow up in finite time), $Ra = 0.7 \times 10^4$.

regions where the behaviour is more complex, period-doublings arise resulting in chaotic responses (Fig. 9). There are also regions of period-three behaviour (Fig. 10) and the subsequent period-doubling to chaos (Fig. 11). This latter feature is new and is not seen in the previous studies [10,11].

Acknowledgements

A. Lazarovici wishes to thank the European Science Foundation REACTOR programme for the grant sponsoring this project, ORS and the University of Leeds for the financial support in the Ph.D. research, and M. Belk for helping with the technical details.

References

[1] N.N. Semenov, Thermal theory of combustion and explosion, Uspekhi Fiz. Nauk. 23 (1940).
[2] R. Aris, The Mathematical Theory of Diffusion and Reaction in Permeable Catalysts. Volume I: The Theory of the Steady State, Clarendon Press, Oxford, 1975.

[3] R. Aris, The Mathematical Theory of Diffusion and Reaction in Permeable Catalysts. Volume II: Questions of Uniqueness, Stability and Transient Behaviour, Clarendon Press, Oxford, 1975.
[4] J. Brindley, N.A. Jivraz, J.H. Merkin, S.K. Scott, Stationary state solutions for coupled reaction–diffusion and temperature-conduction equations. 1. Infinite slab and cylinder with general boundary conditions, Proc. R. Soc. London Ser. A 430 (1990) 459–477.
[5] J. Brindley, N.A. Jivraz, J.H. Merkin, S.K. Scott, Stationary state solutions for coupled reaction–diffusion and temperature-conduction equations. 2. Spherical geometry with Dirichlet boundary conditions, Proc. R. Soc. London Ser. A 430 (1990) 479–488.
[6] B.F. Gray, J.H. Merkin, G.C. Wake, Disjoint bifurcation diagrams in combustion systems, Math. Comput. Modelling 15 (1991) 25–33.
[7] M.A. Sadiq, J.H. Merkin, G.C. Wake, Combustion in a porous material with reactant consumption: the role of the ambient temperature, Math. Comput. Modelling 20 (1994) 27–46.
[8] A.S. Merzhanov, E.A. Shtessel, Free convection and thermal explosion in reactive systems, Astronautica Acta 18 (1973) 191–193.
[9] L. Kagan, H. Berestycki, G. Joulin, G. Sivashinsky, The effect of stirring on the limit of thermal explosion, Combustion Theory and Modelling 1 (1997) 97–111.
[10] T. Dumont, S. Genieys, M. Massot, V. Volpert, Interaction of thermal explosion and natural convection: critical conditions and new oscillating regimes, Equipe d'Analyse Numerique de Lyon (UMR 5585), Preprint 320, 2000.
[11] M. Belk, V. Volpert, Complex dynamics in a problem of heat explosion with convection, submitted for publication.
[12] J. Bebernes, D. Eberly, Mathematical Problems from Combustion Theory, Appl. Math. Sci., vol. 83, Springer-Verlag, New York, 1989.